EasyChair Preprint

№ 15437

Evaluation of Spring Back Phenomenon Existing in Metals: Numerical Modeling and Mathematical Simulations

Elham Abdullah and Abdulkareem Jalil

November 17, 2024

Journal of Mechanical Engineering

Evaluation of Spring Back Phenomenon Existing in Metals: Numerical Modeling and Mathematical Simulations

Elham Abdullah [١], [(*)],Abdulkareem Jaleel[٢]

[١] *Department of Mechanical Engineering; ilham.salman.engh٤٧٩@student.uobabylon.edu.iq ; Faculty of Engineering and Technology; University of Babylon.*

[٢] *Department of Mechanical Engineering; email(٢)@gmail.com; Faculty of Engineering and Technology; University of Babylon.*

(*) Corresponding Author.

ABSTRACT: Spring back phenomenon (SBP) is considered a common issue facing engineers in automotive, ship, and aircraft manufacturing domains reflected in deformations that occur to the metal after the mold loading is removed. For these disciplines, ultimate scales of precision and efficiency in formulating the metal are needed since they cover the outer surface of the mechanical system, like automobiles, ships, and aircrafts. Thus, any small faults or irregularities in the metal's outer surface might be massive if it correspond to larger drag forces and friction affecting the aerodynamic efficiency. Accordingly, this article investigates SBP behaviors in three metals that are exploited heavily in manufacturing, namely aluminum, copper, and pure steel. Corresponding mathematical simulations are implemented by finite element analysis (FEA) in ANSYS®. The core research outcomes revealed that the SBP (elastic recovery percentage) increased after removing the applied mold loading as the punch die radius increases. The SBP relies on the size of the plastic deformation zone. As the punch radius increases, the force spreads to a large plastic area; thus, increasing the SBP. Also, as the punch radius increases, the contact angle and contact area would increase. Hence, SBP could create more friction surface between the punch and the sheet. Pure steel and copper showed larger elastic recovery ratios after removing the mold load than aluminum across all thicknesses. Greater punch radii of the contact area between the punch and the sheet would become greater. Thus, the bending moment would escalate, causing a larger spring back angle. The SBP is much lower in ductile metals than in hard metals because of different Young's modulus.

Keywords: Spring back phenomenon (SBP) • sheet metal forming (SMF) • finite element analysis (FEA) • manufacturing • mold loading • aerodynamic performance.

١. Introduction

Previously, empirical mechanisms were hired to modify process variables until the adverse influences of SBP are minimized. Comparatively, latest manufacturing procedures require significant precision rates of the end-product to provide higher aerodynamic performance of manufactured automotives and aircrafts. Nonetheless, these requirements are not efficient in terms of time, economic profitability, and effort. Subsequently, engineers and researchers conducted extensive research and development (R&D) through experimental works and numerical investigations by simulations to carefully interpret and understand corresponding patterns and mechanical behavior of SBP in metals when a mold load is applied (Broggiato, ٢٠١٢; Xu *et al.*, ٢٠٠٤).

SBP can be explained as a major problem that does frequently take place in sheet metal forming (SMF) processes. It affects end-product's quality, dimensions, and structural integrity. The

elastic recovery of the metal when removing the mold load, i.e., after removing the forming stress can cause the metal to deviate from the planned shape and needed form. The ramifications of such issue may become more complicated since ultimate rates of accuracy and high-performance aerodynamic characteristics are required in these metals, which are exploited in critical manufacturing applications, like automotive, ship, and aerospace (Toros *et al.*, ٢٠١٢).

For this reason, careful understanding of SBP would help engineers create effective strategies to maximize the metals' prediction and metal forming performance within challenging effects of SBP (Chen, ٢٠١١).

Typically, the SMF relies on a punch and a die to shape different metal sheets, creating plastic deformations for necessary shape formulation. Elastic materials can return to their original shape to a partial extent after the mold load is removed. Because of these SBP impacts, metals could not match dimensional tolerances, needing additional processing or adjustments, which result in extra production time and costs To match the increasing requirements correlated with the critical demand for lightweight metals that have complicated geometries to be exploited in many imperative manufacturing domains, like automotive and aerospace, the relevant indices and variables of SBP should be thoroughly inspected (Wu, ١٩٩٦).

٢. Brief Literature Review

Pre-determined SBP simulation optimization sheet metal bending by emergent engineering (Saravanan *et al.*, ٢٠١٨). Most of the impacts of sheet metal thickness, metal sort, tool holder, shank, radius, fraction, friction with shapes, and tie gap on SBP metals have been studied in variable aluminum, copper, and higher strength steels. Their research showed that most variables' effects on this model's formation only SBP on metal deforming. The corresponding optimization process of the SMF variables can be shown in Figure ١.

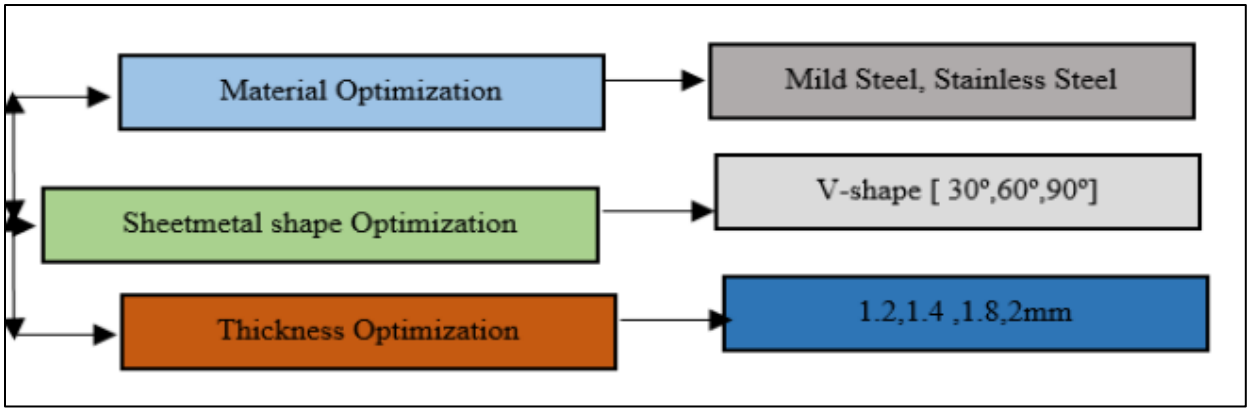

Figure ١. The optimization process of SMF (Saravanan *et al.*, ٢٠١٨).

SBP is the major sheet metal bending flaw. When unloaded, sheet metal bending SBP is elastic. Consider making quality bent sheet metal parts. SBP depends on sheet thickness, tooling geometry, friction, material, and processing parameters. This numerical research examined SBP on edge bending die process. The numerical analysis was done with ANSYS™/ LS-DYNA™. The impacts of sheet metal thickness, type, friction, tool radius, and shape on SBP were studied for aluminum, copper, mild steel, and high-strength steels (Dametew & Gebresenbet, ٢٠١٦).

Also, according to Slota and Jurčišin (٢٠١٢), SMF often experiences SBP due to elastic stress redistribution during unloading. Designing SMF tools needs SBP. Sheet metal V-bending was analyzed using FEA. Transformation Induced Plasticity (TRIP), Advanced High-Strength Steel (AHSS), and mild steel were explored. They considered normal anisotropic material behavior. A practical approach was exploited to develop a contact algorithm for rigid tools of any shape. This paper presented a reliable SBP prediction strategy for sheet bending and unbending. By changing forming procedure operational variables, constitutive models predicted the sheet's final shape after SBP. Experimental and PAM-STAMP ٢G comparisons confirmed the model precision.

Ultrahigh- or high-strength steels could minimize weight and magnify durability but would result in SBP in automobile parts. Most SBP relies on material and part geometry. Extreme deviations from the reference part might exceed the limit. Trial-and-error SBP predictions and deviation corrections are considered laborious. Thus, Baùon *et al.* (٢٠١٦) proposed a novel compensation approach for forming and trimming transfer press-made vehicle part dies.

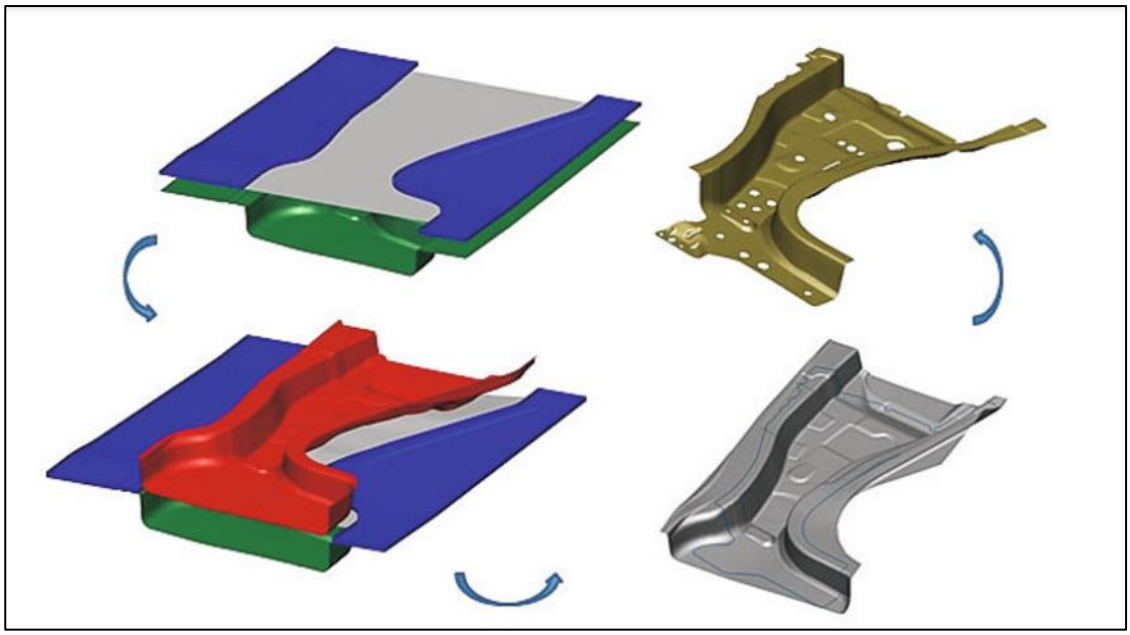

Figure (٢-١): Visualization of simulation process from forming OP-٢٠ to SBP OP-٥٠ (Baùon *et al.*, ٢٠١٦).

The automotive industry is majorly interested in lightweight parts in vehicles. In this context, high-strength aluminum alloys are popular (Choi *et al.*, ٢٠٢٠). High-strength aluminum sheets are hard to form for automotive parts because of their higher strength. Thus, Choi *et al.* (٢٠٢٠) examined ٧٠٧٥ aluminum alloy sheet mechanical properties after W-temper thermal treatment was applied, including a solution of thermal treatment and quenching.

The influence linked to the damping rate, integration points, number of blank meshing scale, and punch speed on the precision and performance of SBP mathematical simulations were investigated. Then, reasonable values were proposed, relying on the U-bending procedure. NUMISHEET'٩٣ is a one example of the benchmarks (Xu *et al.*, ٢٠٠٤).

Asgari *et al.* (٢٠٠٨) created a statistical strategy to examine TRansformation Induced Plasticity (TRIP) in forming and SBP problems relying on an industrial case study. The statistical significance of the chosen variables for forming and SBP prediction were discussed as well. Changes of up to ±١٠٪ in Young's modulus and friction coefficient did not remarkably influence SBP precision and SBP statistical correlations. Figure ٢ shows SBP measurement points (A١–E٢) and constraint points (P١–P٤).

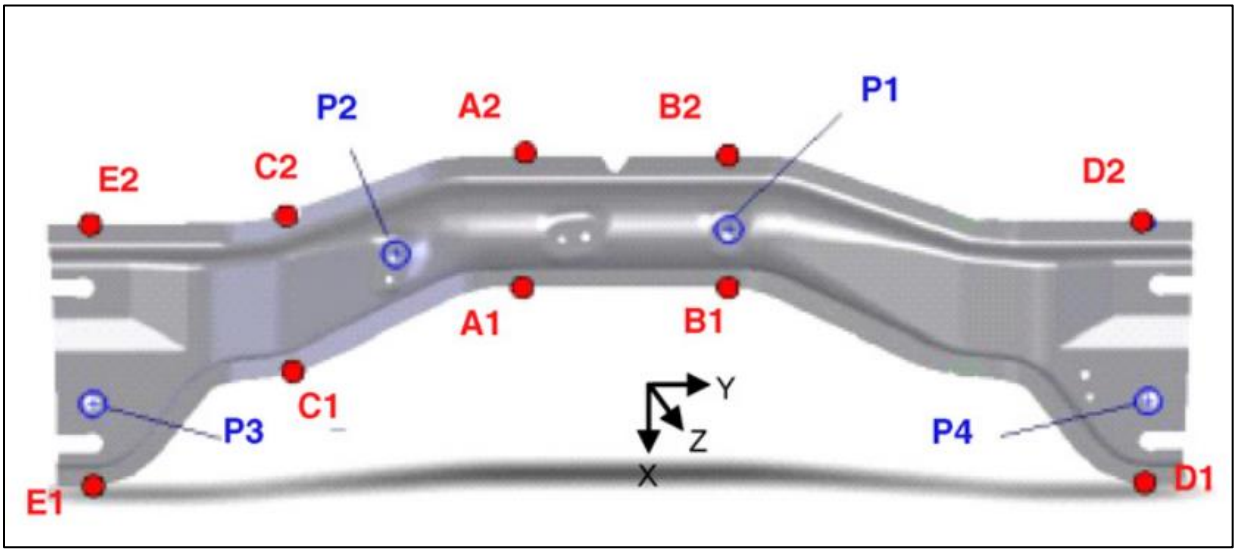

Figure ٢. SBP measurement points (A١–E٢) and constraint points (P١–P٤) (Asgari *et al.*, ٢٠٠٨).

SBP-strain recovery after forming loads are removed—is a major issue in SMF (Vrh *et al.*, ٢٠٠٩). Controlling this problem requires physically exact numerical modeling of the forming procedure and SBP mathematical simulations. Existing mechanisms could not precisely forecast and identify SBP. The researchers in this work built a constitutive model for metal forming, which accounts for sheet anisotropy, damage evolution, and strain path-dependent stiffness degradation.

In conclusion, after reviewing some studies on SBP in manufacturing disciplines, it is imperative to point out that the major objective of this paper is inspired from these current challenges to investigate the major trends, patterns, and mechanical behaviors of the three most prevalent metals exploited in various manufacturing fields, mainly vehicles, to upgrade the scales of accuracy and performance of the SMF and overcome and alleviate the harmful effects of the SBP.

Since experimental approaches are expensive and greatly exposed to errors, numerical analysis and mathematical modeling and advanced simulations can provide clearer outcomes through efficient software tools would be remarkably practical because the boundary conditions and constraints of the problem can be controlled straightforwardly. Also, time limitations linked to comprehensive tests might hinder the implementation of experimental approaches.

The sequence of this paper can be explained in the following:

- **Section ٣** expresses the paper's materials and methods,

- **Section ٤** indicates the paper's numerical analysis, modeling, and mathematical simulations,
- **Section ٥** explains the major research outcomes,
- **Section ٦** gives a summary of the research outcomes in the conclusions part,
- **Section ٧** displays the future research directions.

٣. Materials and Methods

This study is conducted to bridge a knowledge gap reflected in the need for abundant discussions and data on numerical analysis, modeling, and mathematical simulations of metals exploited in the context of SMF in manufacturing vehicles, aircrafts, and ships instead of time-consuming and low accurate tests considered in experimental investigation contexts.

It is expected from implementing the numerical research by the FEA in the ANSYS software tool that this study will answer the following questions:

- What are the major variables, constraints, and boundary conditions that influence the expansion and occurrence of SBP to be considered in the FEA?
- What are the better strategies and approaches to minimize this harmful problem in metals while they are processed in SMF?
- Which metals among the three (Al, Cu, and Fe) would show more stable mechanical deformation behaviors and strain trends after applying the FEA?

FEA expresses a popular numerical strategy to simulate metal's behavior and process conditions. Many numerical models can be calibrated and modified in computer platforms, eliminating the need for challenging experimental data, which may correspond to extensive costs, efforts, and time because of lengthy and frequent tests. The numerical procedure across which this research will pass can be shown in Figure ٣.

٤. Numerical Modeling and Mathematical Simulation Procedures

Before starting the numerical investigation process, the necessary shapes, and designs of the samples under the dimensions and geometric forms used in the laboratory are formulated and created in the SolidWorks® Software. The models can be then exported to the computer program in which mathematical simulations are performed to predict the crucial mechanical properties and other characteristics when they are subjected to certain static loads.

٤,١ *Software Package*

The software computer platform harnessed in this paper is the ANSYS® Software Package. It is the most popular program involved in numerical modeling and mathematical simulations, enabling scholars to perform precise evaluations, analyses, and explorations of variant categories of mathematical problems in mechanical engineering and manufacturing efficiently, providing a time, effort, and cost efficiencies than traditional experimental approaches that may be difficult-to-implement in some situations or they might be expensive and lengthy.

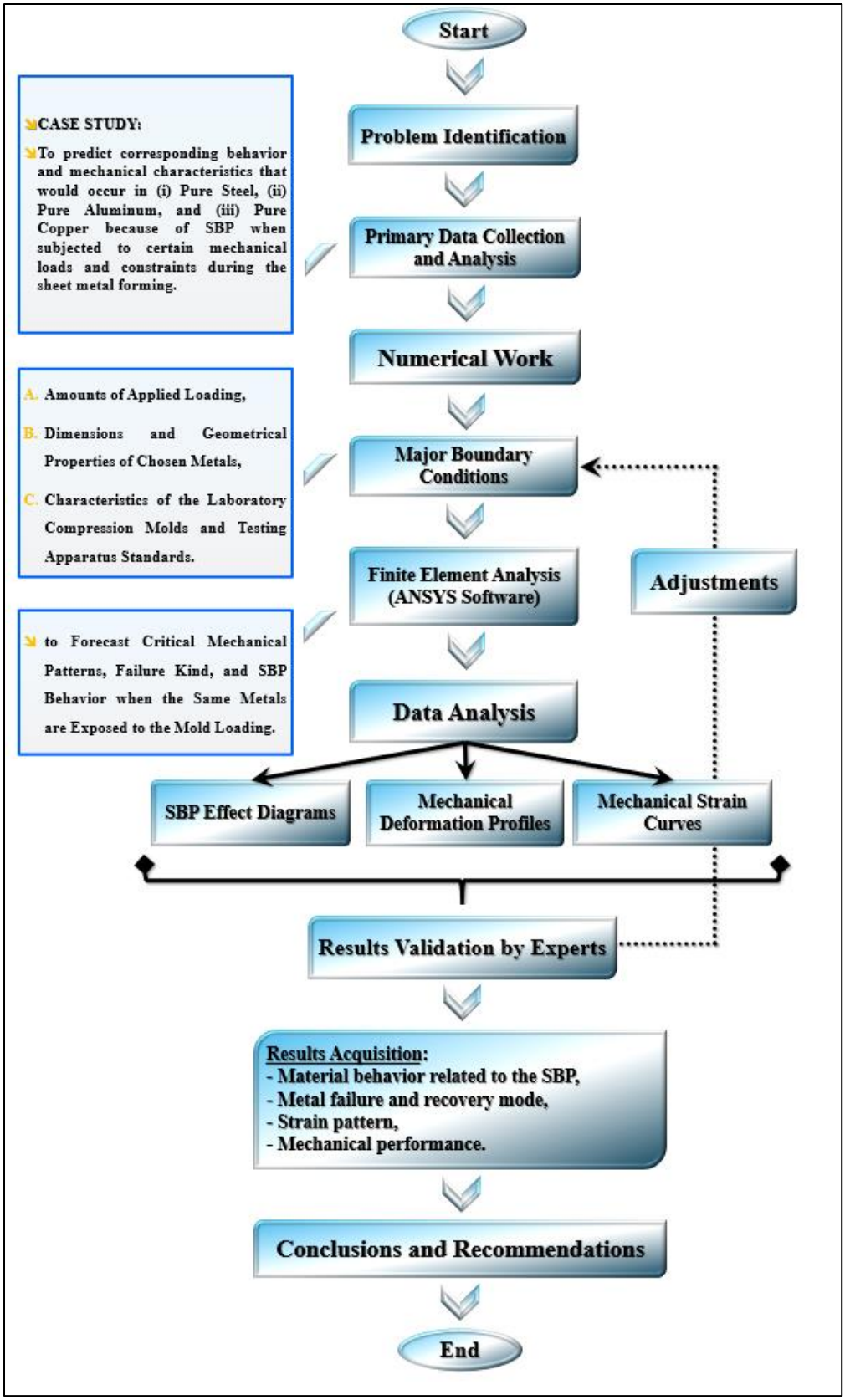

Figure ٣. The research method flowchart related to this article (The researcher, ٢٠٢٤).

As explained earlier, the current research will examine the SBP behavior in three commonly exploited metals in automotive and aerospace, namely pure aluminum, copper, and pure steel. These materials have distinctive mechanical features including yield strengths and elastic moduli that affect SBP behavior (Broggiato, ٢٠١٢; Katre *et al.*, ٢٠١٥).

Additionally, ANSYS allows investigators to choose numerous sorts of materials and metals, identify their physical and mechanical characteristics, choose major amounts, types, and directions of loads, and distinguish other crucial boundary constraints. After that, corresponding meshing procedures are implemented to facilitate the mathematical simulations, helping provide ultimate scales of simulation and numerical analysis efficiency and performance. After running the mathematical simulations, relevant numerical outputs are obtained.

٤,٢ *The Meshing Process*

The meshing process is one of the critical phases that are carefully implemented to make sure precise numerical outcomes and high-quality results are attained. The meshing task can start with studying the kind of structure. It can be considerably simple in some mechanical problems, like circular-cross-section beams, rectangular parallelepiped mechanical problems, and square-like top and side faces of materials (Guo *et al.*, ٢٠٢١).

Simultaneously, mechanical structures, in some conditions, might be remarkably sophisticated, as they express larger mechanical structures introduced in real-life manufacturing disciplines, like vehicles, ships, or aircrafts.

For these complex objects, adopting mathematical simulations would not give accurate results because of many faults and errors when exploiting a simple design that expresses the whole vehicle body of the automobile, ship, or the aircraft. As a result, low-quality outcomes and low-performance predictions of the mechanical behavior would be reached (Jin *et al.*, ٢٠٢١).

To overcome this barrier, researchers considered dividing the whole complicated structure into small elements/ cells, whose dimensions, general geometry, and mechanical properties are very simple, enabling remarkably mathematical simulation flexibility and straightforward numerical analysis, which can supply substantially exact outputs. These elements shape well-known mathematical shapes, such as cubes, prisms, tetrahedral components, polygonal shapes, and many plain engineering shapes. After choosing the proper simple shape, the meshing process can be initiated by identifying the overall number of these simple geometric shapes that form the whole complicated shape (Pagani *et al.*, ٢٠٢١).

Nevertheless, researchers should carefully choose the optimum overall number of these cells/ elements since massive number of simple elements could affect the simulation process and make it remarkably challenging in terms of time consumption, computational complexity, and cost (Szabó and Babuška, ٢٠٢١).

Concerning the meshing procedure and the whole shape division linked to the three specimens (Al, Cu, and Fe) built and modeled in the SolidWorks® platform, Table ١ shows critical meshing variables, and their corresponding values exploited in this simulation work.

Table ١. Major meshing characteristics of the three metals investigated numerically.

No.	Category	Amount/ Clarification
١	**Type of the Chosen Cell**	**XXXX**
٢	**Dimensions of the Geometric Shape**	**XXXX**
٣	**The Overall Number of Meshing Elements**	**XXXX**

٤,٣ *Finite element analysis (FEA)*

Finite element analysis (FEA) is a breakthrough analytical tactic created by researchers for the aim of identifying a number of significant in metals, materials, and engineering structures, which have very complicated designs and cannot be flexibly investigated relying on conventional solutions and experimental approaches. Mechanical engineering problems, which are nonlinear, very sophisticated, and they are time, cost, and effort consuming when they are explored can be straightforwardly inspected relying on FEA principles. FEA can allow scholars to predict and foresee various mechanical properties of these complicated structures and predict their failure trend, deformation behavior, and stress and stress patterns when they are subjected to static, dynamic, or thermal loads. FEA results can reach very precise scales because many boundary conditions and constraints can be easily identified and distinguished for the problem, like current temperature, dimensions, geometrical conditions, pressure, and many more variables. It can predict difficult-to-identify features because of numerous complexities and uncertainties related to the material behavior and mechanical patterns that would largely vary when loads are implemented. FEA can offer cost-effective numerical modeling and investigation solutions through precise mathematical simulations, replacing costly and inefficient traditional investigation mechanisms (Kurowski, ٢٠٢٢).

Finite Element Analysis (FEA) and other numerical methods are widely used to simulate and forecast SBP. These approaches often need aid to examine material behavior's complexity under different forming conditions. These simulations depend on right input data, including material properties and numerical techniques (Helmy, ٢٠١٩; Jiang and Li, ٢٠١٥; Kim *et al.*, ٢٠١٠).

٤,٤ *Major Properties of the Three Investigated Materials*

The numerical investigation approach is conducted to examine the behavior of the three major materials (Al, Cu, Fe). Fe corresponds to the pure steel since there are many types of iron. Table ٢ distinguishes the critical properties of these three materials. Most of these variables and their corresponding values will be exploited for the identification of the boundary conditions linked to the three explored metals.

Table ٢. Critical common mechanical and physical properties of the three inspected metals.

No.	Mechanical and Physical Properties	Metal Name		
		Pure Steel	Pure Aluminum	Pure Copper
١	**Color**	Gray	Silvery-White	Red-Orange
٢	**Density**	٧,٨٥٠ kg/m^٣	٢,٧٠٠ kg/m^٣	٨,٩٢٠ kg/m^٣
٣	**Tensile Strength**	٤٢٠ MPa	٩٠ MPa	٢٠٠ to ٣٦٠ MPa
٤	**Modulus of Elasticity/ Young's Modulus**	٢٠٠ GPa	٦٨ GPa	١٢٠ GPa
٥	**Shear Modulus**	٨٠ GPa	٢٥ GPa	٤٤ Gpa
٦	**Poisson's Ratio**	٠,٢٥	٠,٣٦	٠,٣٥
٧	**Melting Temperature Point**	١,٢٠٥ °C to ١,٣٧٠ °C	٦٦٠ °C	١,٠٨٣ °C
٨	**Thermal Conductivity**	٤٤ to ٥٢ W/m.K	٢٣٧ W/m.K	٢٦٠ W/m.K
٩	**Vickers Hardness**	١٢٦ HV	١٥٠ to ١٦٠ HV	٤٠ to ١١٠ HV

٥. Critical Numerical Simulation Outputs

٥,١ *Models and Mold Mechanical Design*

After performing the mathematical simulation process and numerical modeling and analysis, some critical graphical data were obtained. For example, Figure ٤ expresses ٣D models of the three aluminum specimens created for the numerical mechanical analysis of thicknesses of ٢ ± ٠,١٣ mm and (a) punch radius of ٢,٠ mm and a bend angle of ٩٢,٤٢° ± ٠,٥٠°, (b) punch radius of ٣,٥ mm and a bend angle of ٩٢,٦٢° ± ٠,٥٠°, and (c) punch radius of ٤,٠ mm and a bend angle of ٩٣,٢٦° ± ٠,٥٠°.

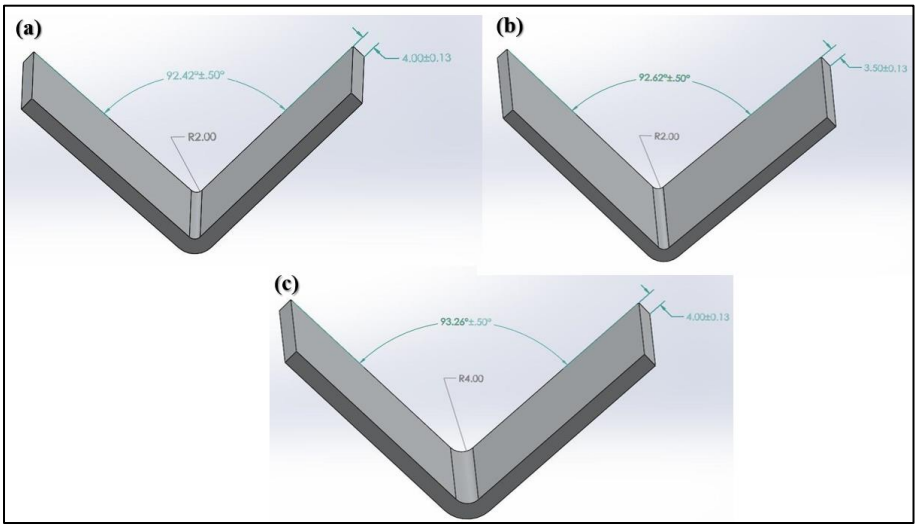

Figure ٤. ٣D models of the aluminum specimens of various thicknesses, punch radiuses, and bend angles.

Similarly, Figure ٥ indicates these values for the copper specimens.

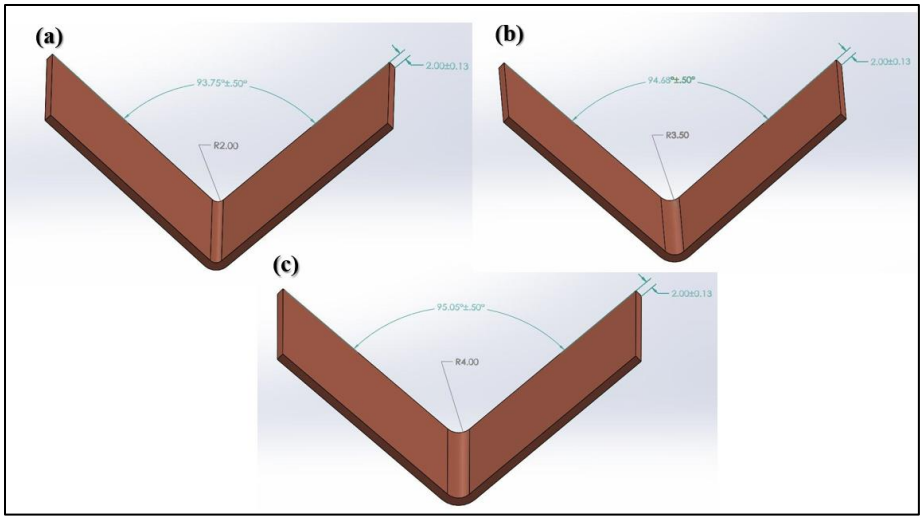

Figure ٥. ٣D models of copper specimens of various thicknesses, punch radiuses, and bend angles.

It can be inferred from Figure ٥ that the ٣D models of the copper specimens created for the numerical mechanical analysis have different dimension. All three specimens have thicknesses of ٢ ± ٠,١٣ mm. The first one has a punch radius of ٢,٠ mm, and a bend angle of ٩٣,٧٥° ± ٠,٥٠°. The second specimen has a punch radius of ٣,٥ mm and a bend angle of ٩٤,٦٨° ± ٠,٥٠°. The third specimen has a punch radius of ٤,٠ mm and a bend angle of ٩٥,٠٥° ± ٠,٥٠°. Figure ٦ displays the three pure steel specimens.

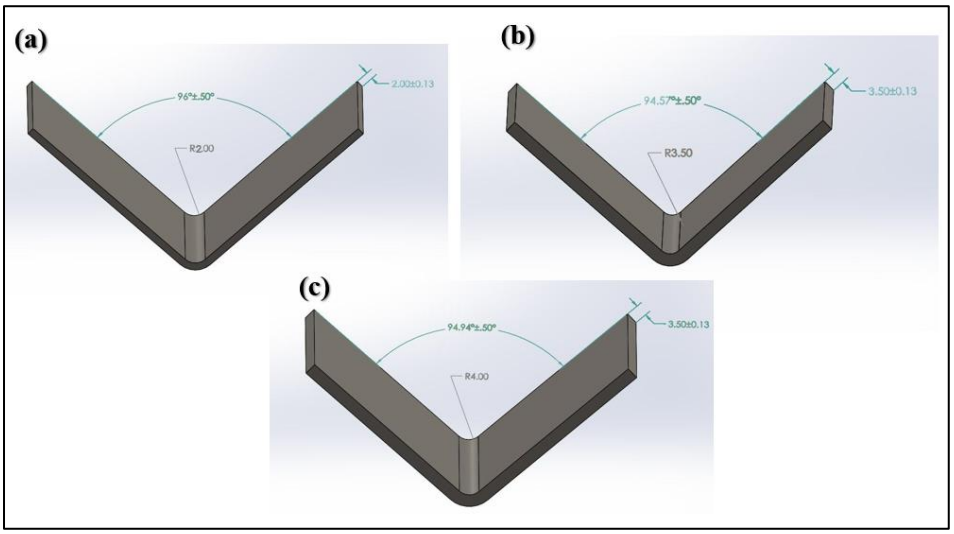

Figure ٦. ٣D models of pure steel specimens of various thicknesses, punch radiuses, and bend angles.

It can be inferred from Figure ٦ that the ٣D models of the pure steel specimens created for the numerical mechanical analysis have various dimensions. The first one has a thickness of ٢,٠ ± ٠,١٣ mm, punch radius of ٢,٠ mm, and a bend angle of ٩٦,٠٠° ± ٠,٥٠°. The second sample has a thickness of ٣,٥ ± ٠,١٣ mm, a punch radius of ٣,٥ mm, and a bend angle of ٩٤,٥٧° ± ٠,٥٠°. The third one has a thickness of ٣,٥ ± ٠,١٣ mm, a punch radius of ٤,٠ mm, and a bend angle of

٩٤,٩٤° ± ٠,٥٠°. The molds created to apply necessary mold loading in the SMF process can be shown in Figure ٧.

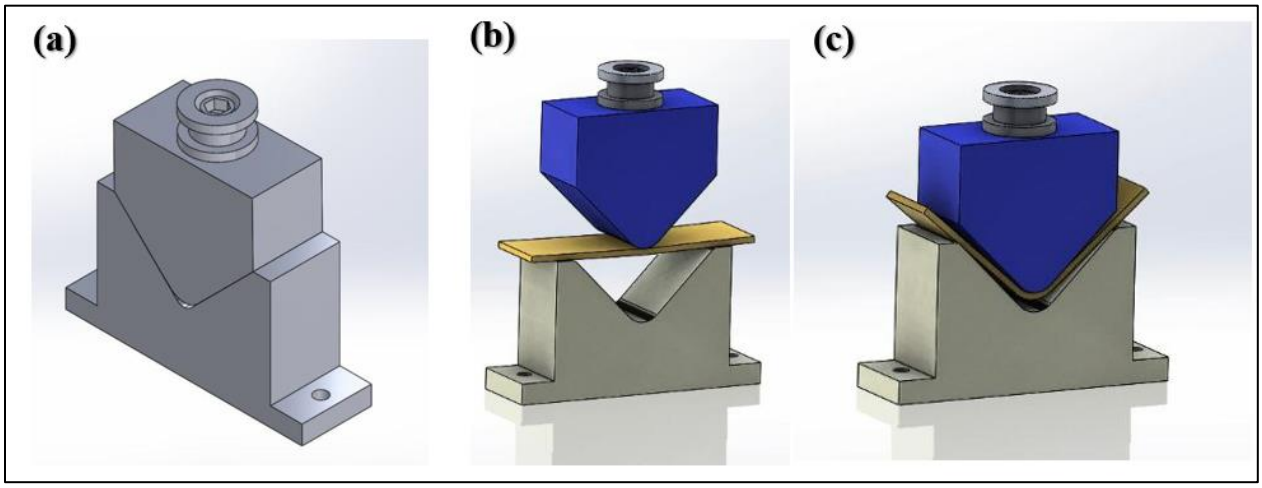

Figure ٧. Configurations of (a) the ٣D numerical mold, (b) a copper specimen to be bended by the mold, and (c) bended Cu specimen.

It can be noted from Figure ٧ that the ٣D mold exploited in this study has a V-shape. Deformations occurred to this copper specimen after applying the load are shown in Figure ٧, c.

٥,٢ *Numerical Simulation Outcomes*

The numerical ANSYS results also revealed some outcomes regarding the six specimens (two for each Al, Cu, and pure Fe). These results can be shown in Table ٣.

Table ٣. The numerical outcomes of the strain analysis of the six samples.

Time (Seconds)	Strain Rate (Cu [١])	Strain Rate (Cu [٢])	Strain Rate (Al [١])	Strain Rate (Al [٢])	Strain Rate (Fe [١])	Strain Rate (Fe [٢])
٠,١٦	٠,٠٦١٢٥	٠,٠٧٢٥٠	٠,٠٤٥٠٠	٠,٠٥٨٧٥	٠,٠٤٠٠٠	٠,٠٤١٢٥
٠,٢٤	٠,٠٦١٢٥	٠,٠٧٣٧٥	٠,٠٤٣٧٥	٠,٠٥٨٧٥	٠,٠٤٠٠٠	٠,٠٤١٢٥
٠,٣٢	٠,٠٦١٢٥	٠,٠٧٢٥٠	٠,٠٤٥٠٠	٠,٠٥٨٧٥	٠,٠٤٠٠٠	٠,٠٤١٢٥
٠,٤٠	٠,٠٦١٢٥	٠,٠٧٢٥٠	٠,٠٤٣٧٥	٠,٠٦٠٠٠	٠,٠٤٠٠٠	٠,٠٤١٢٥
٠,٤٨	٠,٠٦١٢٥	٠,٠٧٢٥٠	٠,٠٤٥٠٠	٠,٠٥٨٧٥	٠,٠٤٠٠٠	٠,٠٤١٢٥
٠,٥٦	٠,٠٦١٢٥	٠,٠٧٣٧٥	٠,٠٤٣٧٥	٠,٠٥٨٧٥	٠,٠٤٠٠٠	٠,٠٤١٢٥
٠,٦٤	٠,٠٦١٢٥	٠,٠٧٢٥٠	٠,٠٤٥٠٠	٠,٠٥٨٧٥	٠,٠٤٠٠٠	٠,٠٤١٢٥
٠,٧٢	٠,٠٦١٢٥	٠,٠٧٢٥٠	٠,٠٤٣٧٥	٠,٠٥٨٧٥	٠,٠٤٠٠٠	٠,٠٤١٢٥
٠,٨٠	٠,٠٦١٢٥	٠,٠٧٢٥٠	٠,٠٤٥٠٠	٠,٠٥٨٧٥	٠,٠٤٠٠٠	٠,٠٤١٢٥
٠,٨٨	٠,٠٦١٢٥	٠,٠٧٢٥٠	٠,٠٤٣٧٥	٠,٠٥٨٧٥	٠,٠٤٠٠٠	٠,٠٤١٢٥
٠,٩٦	٠,٠٦١٢٥	٠,٠٧٣٧٥	٠,٠٤٥٠٠	٠,٠٥٨٧٥	٠,٠٤٠٠٠	٠,٠٤١٢٥
١,٠٤	٠,٠٦١٢٥	٠,٠٧٢٥٠	٠,٠٤٣٧٥	٠,٠٥٨٧٥	٠,٠٤٠٠٠	٠,٠٤١٢٥
١,١٢	٠,٠٦١٢٥	٠,٠٧٢٥٠	٠,٠٤٥٠٠	٠,٠٥٨٧٥	٠,٠٤٠٠٠	٠,٠٤١٢٥
١,٢٠	٠,٠٦١٢٥	٠,٠٧٢٥٠	٠,٠٤٣٧٥	٠,٠٥٨٧٥	٠,٠٤٠٠٠	٠,٠٤١٢٥

To explain the relevance and importance of these findings, corresponding graphical plots were created. Figure ٨ displays a comparative analysis concerning the variation of strain of the six specimens (two in each of Al, Cu, and pure Fe) with respect to the time.

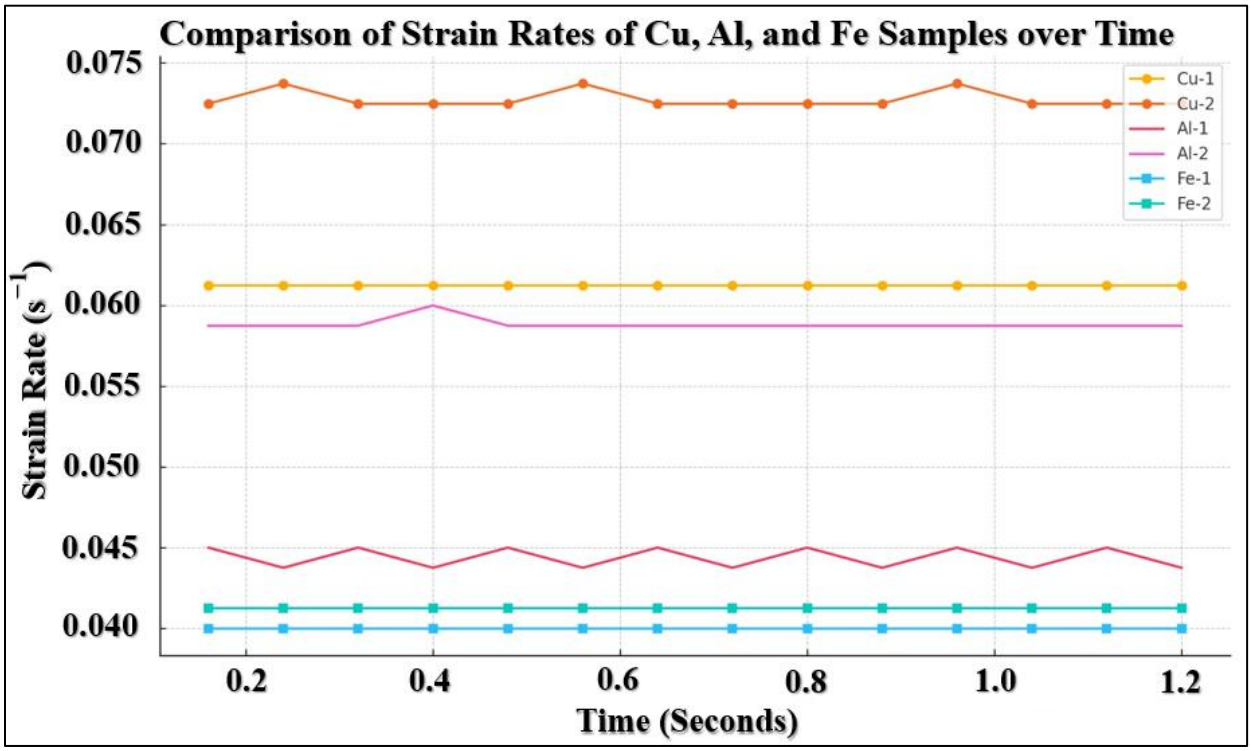

Figure ٨. The numerical results of the strain profile of the six investigated samples.

It can be inferred from Figure ٨ that the second copper specimen has the highest rates of strain compared with other specimens (accounting to approximately ٠,٠٧٣ across the numerical simulated time), followed by the first copper specimen (٠,٠٦٢ along the whole simulated time), which is followed by second aluminum specimen (٠,٠٥٨٥). In contrast, the lowest strain rates were noted in the first and second pure steel specimens, accounting to ٠,٠٤٠ and ٠,٠٤١, respectively. The first aluminum specimen, which is lighter than pure steel and is remarkably practical for manufacturing light-weight vehicles has a very closer strain rate to the two pure steel specimens, whose strain rate reached ٠,٠٤٥.

In addition, referring to the numerical simulation results expressed in Table ٣, relevant graphical illustrations can be expressed in Figure ٩. Specifically, this figure indicates the variation of the strain of the three metals with the load application time.

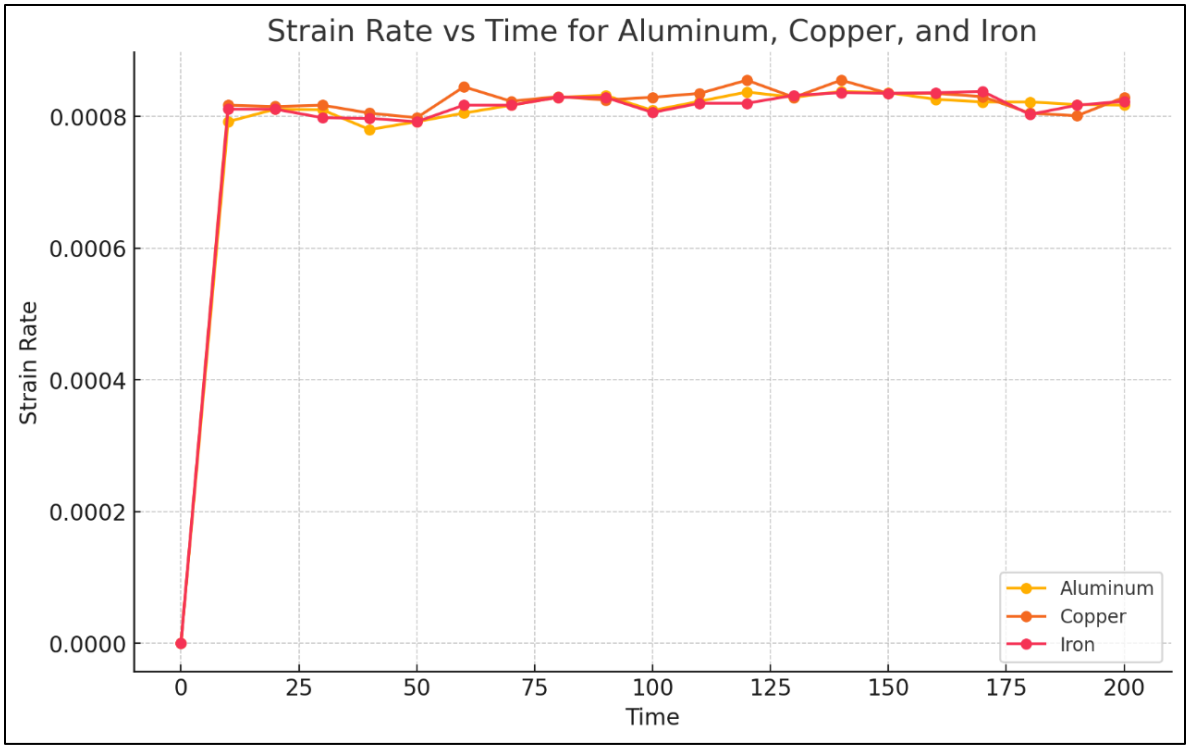

Figure ٩. The strain rate of the three investigated metals with the load application time.

It can be inferred from the outcomes illustrated in Figure ٩ that there is a dramatic increase in the strain rate at the first intervals of the load application time, which indicates similar rapid response to the load among the three metals. Then, after about ١٣ seconds, the three strain rate profiles would show more stability fluctuating around a steady strain value, which is about ٠,٠٠٠٨ across the rest of the load application time.

Accordingly, a conclusion can be reached regarding the SBP behavior among aluminum, copper, and pure steel, translated in the large similarity of SBP pattern, which shows substantial and abrupt response to the load, which becomes more stable after a certain portion of time. These observations are the same in the three investigated metals, which can enable their exploitation in certain manufacturing scenarios under which loads are applied and considered.

The results also revealed the kind of the deformation behaviors among the three investigated metals with the load application time, which can be expressed in Figure ١٠.

Journal of Mechanical Engineering

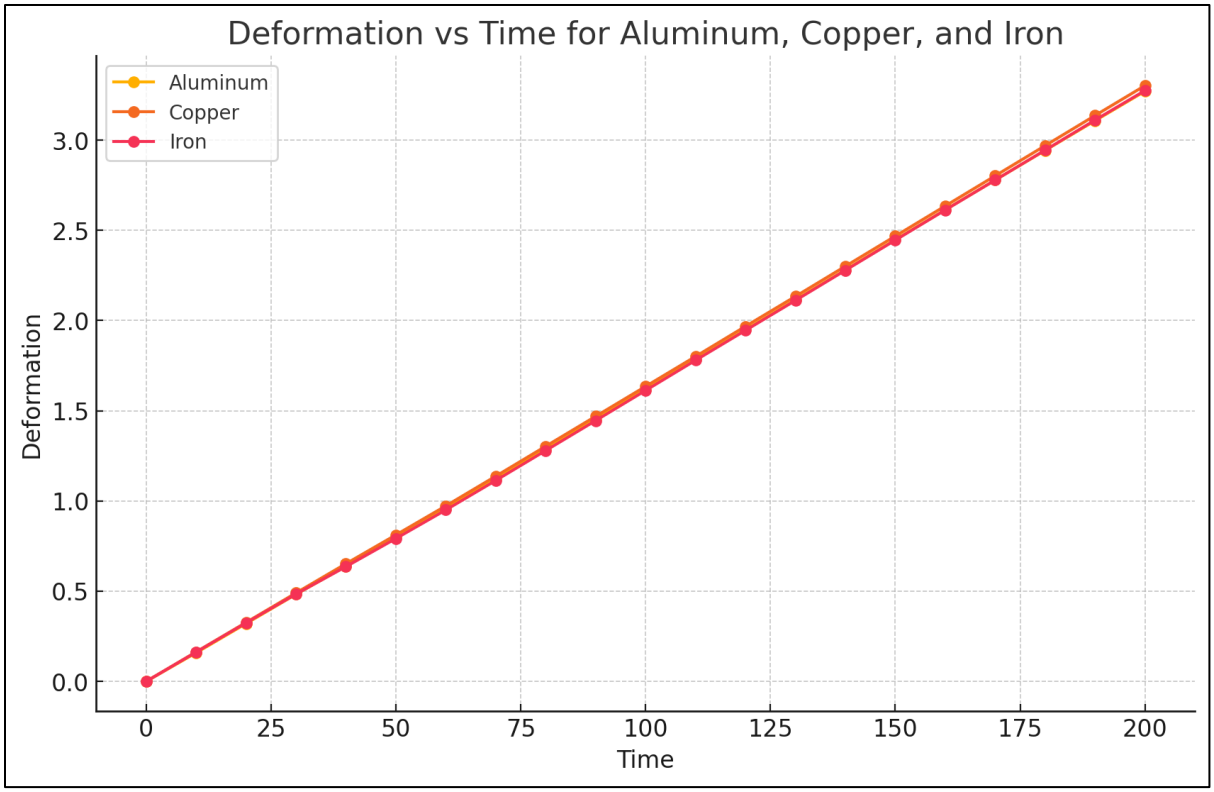

Figure ١٠. Deformations of the three investigated metals with the load application time.

It can be concluded from Figure ١٠ that deformations increase linearly with the load application time, which is greatly similar to the three metals. This fact can clarify that aluminum, copper, and pure steel have larger behavior in terms of the deformation change respecting to the time. The simulation results provided data on the SBP of the aluminum specimens (Figure ١١).

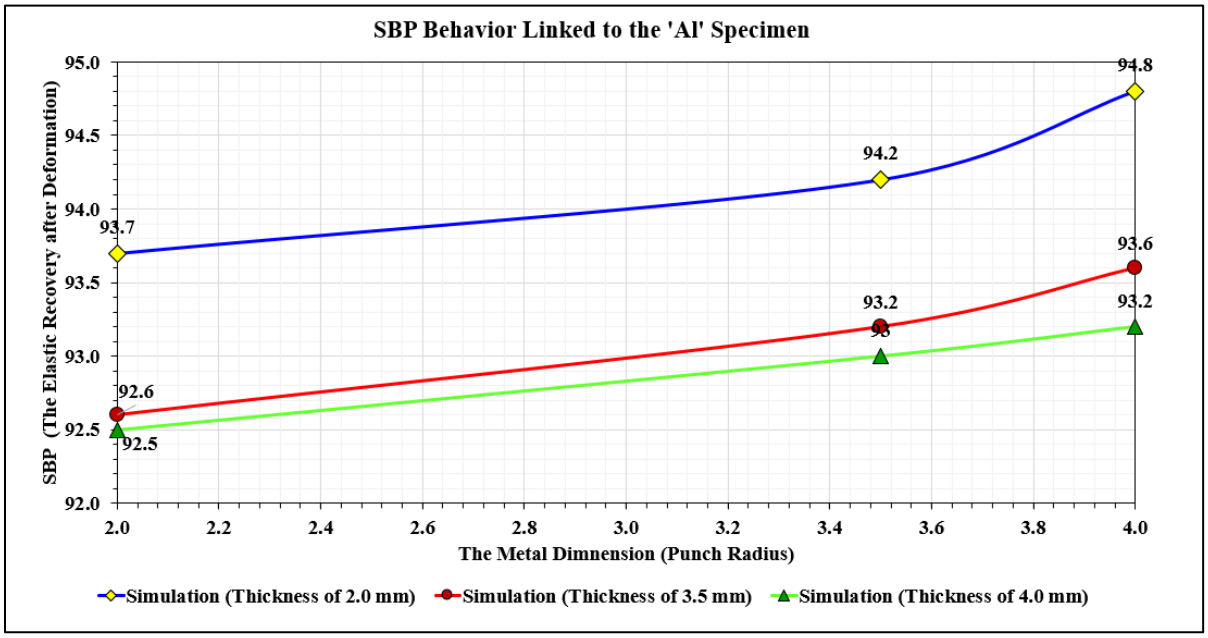

Figure ١١. The SBP results from the simulation outcomes of the three aluminum samples.

It can be concluded from the outcomes shown in Figure ١١ that the behavior correlated with the SBP would rise with respect to the metal dimension (the radius of punch). Those aluminum specimens with lower thicknesses would have greater effects and notable SBP impacts compared with aluminum specimens with more thickness. The deformation is observed to increase with more metal thickness.

Figure ١٢ displays the behavior of the SBP from the numerical simulation outcomes of the three copper specimens with three thicknesses.

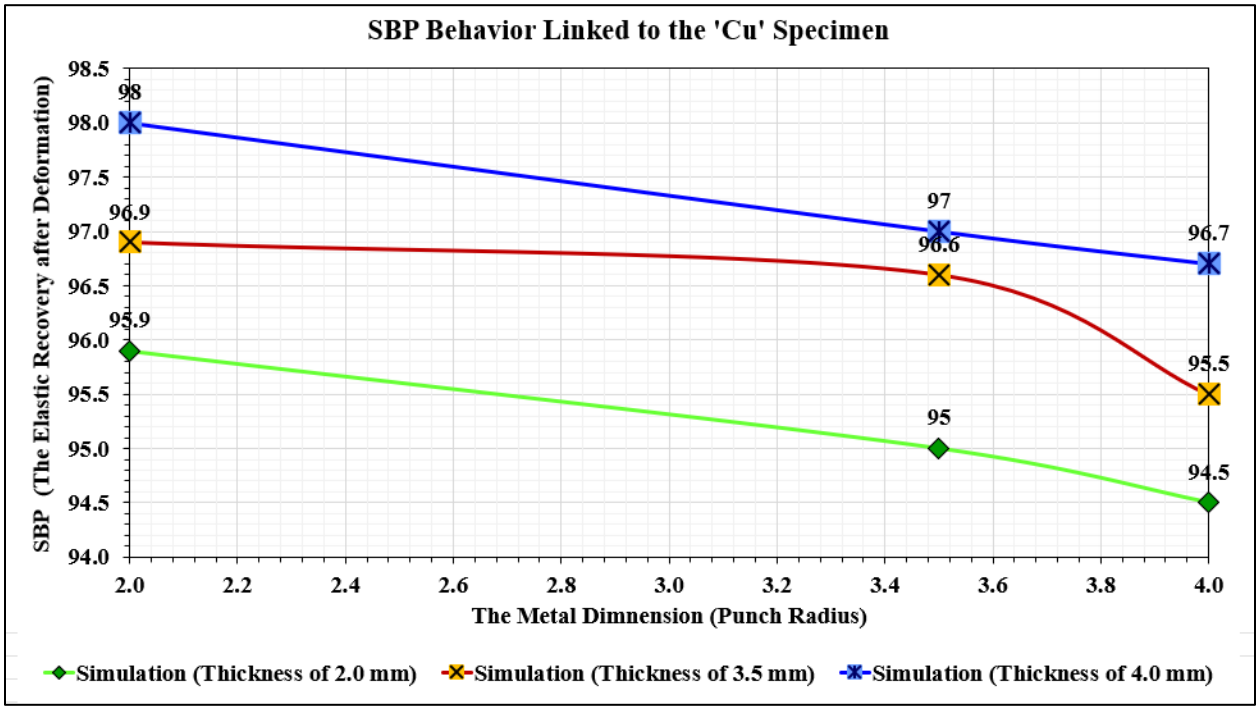

Figure ١٢. The behavior of the SBP from the numerical simulation outcomes of the three copper specimens with three thicknesses.

It can be understood from the numerical outcomes expressed in Figure ١٢ that the behavior pertaining to the SBP would record small reduction with respect to the metal dimension (the punch radius). Copper specimens with larger thickness were noted to have higher SBP and elastic recovery after deformation compared with those ones that have lower thicknesses. As a result, the copper deformation would record higher rates with larger thicknesses but less values with more significant punch radius rates.

Similar to aluminum and copper, Figure ١٣ shows the behavior of SBP under various punch radius rates of three pure Fe specimens with different thicknesses.

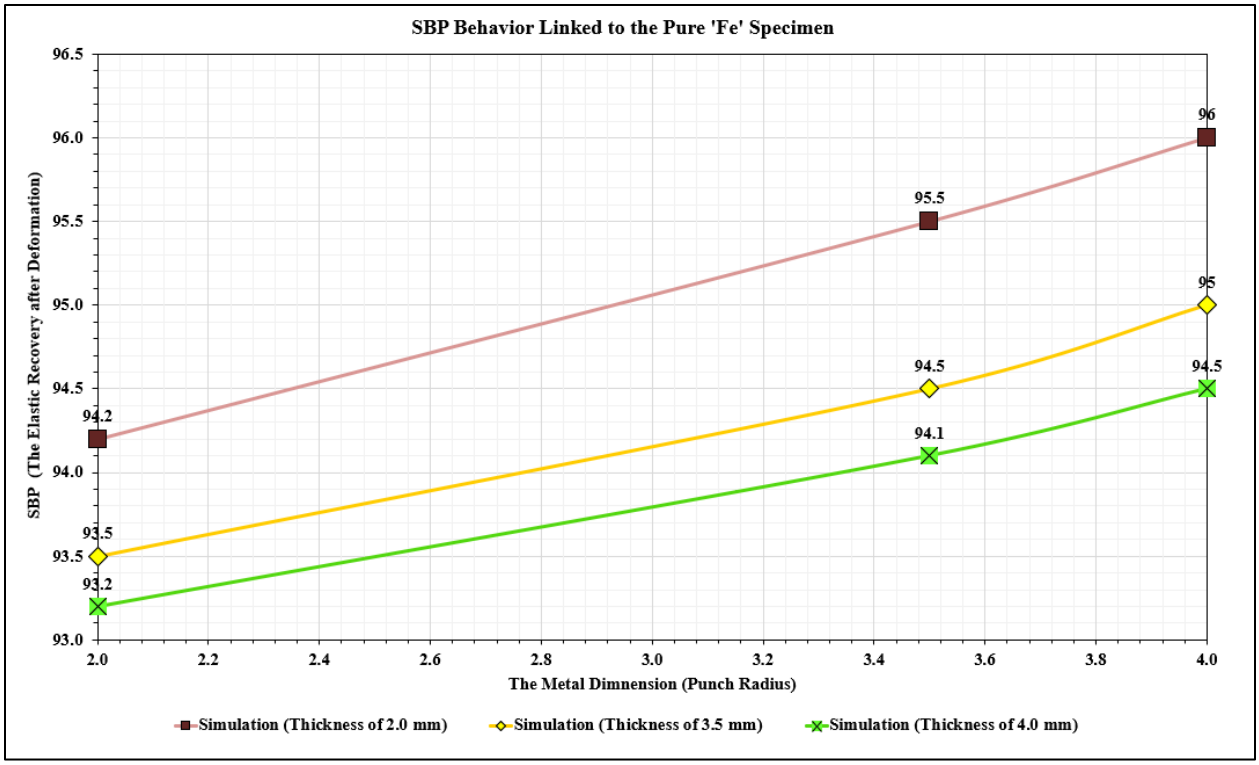

Figure ١٣. The behavior of the SBP from the numerical simulation outcomes of the three pure steel specimens with three thicknesses.

It can be realized from the numerical outcomes illustrated in Figure ١٣ that the pattern respecting the SBP in the three pure steel tends to rise with larger values of punch radius. In addition, it can be noted that pure steel specimens that have lower thicknesses have more significant effects and observations of SBP compared with other pure Fe specimens with higher thicknesses.

As a conclusion, it can be said that pure steel specimens, which have less thicknesses would be remarkably influenced by SBP compared with specimens with higher thicknesses. Additionally, larger punch radius rates would cause more realized occurrence of the SBP.

٥,٣ *Comparative Analysis of the SBP between the Three Metals*

To provide means of comparison and better understanding concerning which metal would respond effectively or poorly to the mold loading and cause lower or larger deformations and harmful effects due to SBP, respectively, some graphical plots were created. Figure ١٤ expresses the SBP behavior (the elastic recovery ratio) of the three metals of a thickness of ٢,٠ mm.

It can be inferred from the graphical comparative analysis in Figure ١٤ that the numerical results proved that the pure steel specimens of a thickness of ٢,٠ mm showed more significant elastic recovery after deformation (higher values of SBP), compared with copper and aluminum. Comparatively, the aluminum specimens have lower elastic recovery after removing the mold load. However, copper did approximate the aluminum behavior at a thickness of ٢,٠ mm. Both had an elastic recovery of ٩٣,٧٪. Nonetheless, pure steel still has the highest elastic recovery

compared to the two metals. It reaches its maximum elastic recovery ratio (٩٦,٠٪) when the specimen thickness of ٤,٠ mm.

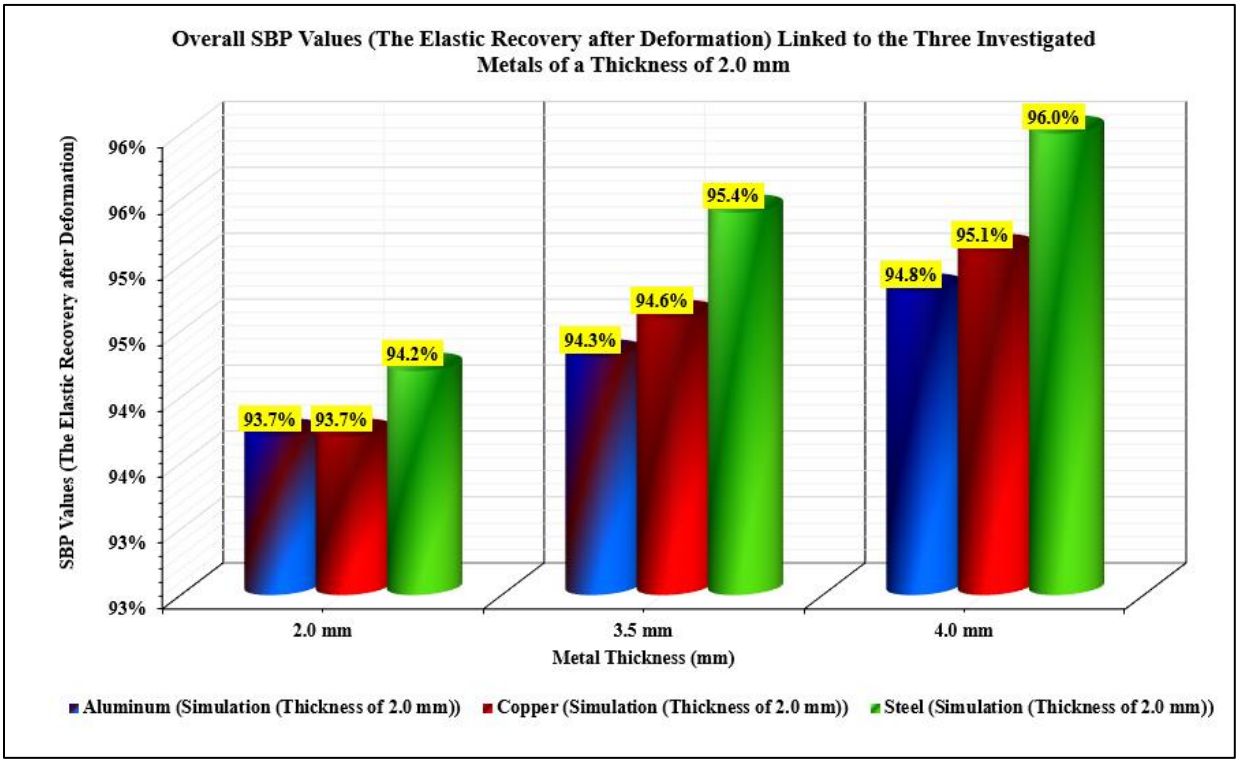

Figure ١٤. The SBP behavior (the elastic recovery ratio) of the three metals of a thickness of ٢,٠ mm.

Accordingly, it can be said that the pure steel consistently exhibits the highest elastic recovery (SBP) rate across all metal thicknesses, while aluminum shows the lowest values, except at ٢,٠ mm where it ties with copper. In conclusion, the graph highlights the superior elastic recovery of steel in deformation conditions compared with the other two metals.

Concerning the specimens' thickness of ٣,٥ mm, Figure ١٥ expresses the percentage of the elastic recovery of the three metals with varying thicknesses after the applied mold load was removed through numerical simulations.

It can be realized from the graphical comparative analysis shown in Figure ١٥ that the numerical results confirmed that, again, the pure steel specimens of a thickness of ٣,٥ mm did show more remarkable elastic recovery percentage after deformation compared with copper and aluminum. In contrast, the aluminum specimens have lower elastic recovery after removing the mold load (٩٢,٦٪ at a thickness of ٢,٠ mm). Copper was closer to the aluminum elastic recovery behavior at a thickness of ٢,٠ mm (٩٢,٨٪). Nonetheless, pure steel still record the highest elastic recovery ratio compared with those two metals. It reaches its maximum elastic recovery ratio (٩٥,٠٪) when its specimen thickness was ٤,٠ mm.

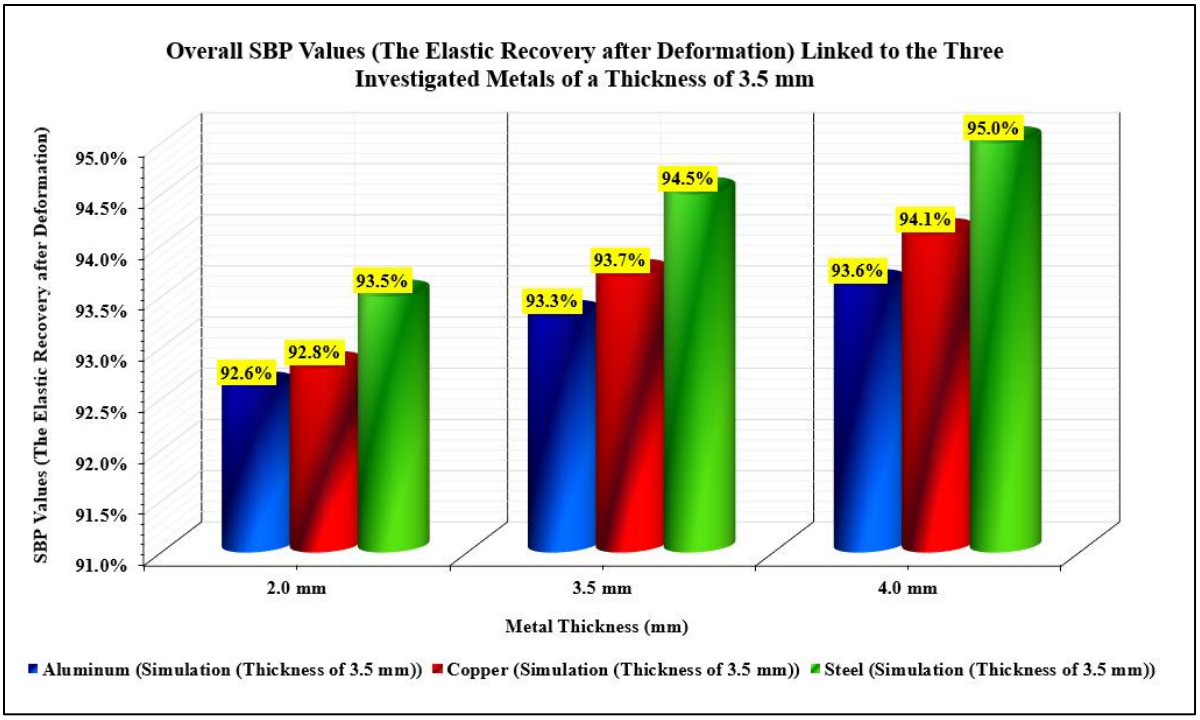

Figure ١٥. The SBP (the elastic recovery ratio) of the three metals of a thickness of ٣,٥ mm.

As a whole, it can be concluded that the steel consistently exhibits the highest elastic recovery (SBP) proportion across all metal thicknesses, while aluminum shows the lowest values, except at ٢,٠ mm where it ties with copper. Therefore, Figure ١٥ proves the superior elastic recovery of steel in deformation conditions compared with the other two metals.

Concerning the specimens' thickness of ٤,٠ mm, Figure ١٦ expresses the outcomes of the ratio of the elastic recovery of the three metals of varied thicknesses after removing the load.

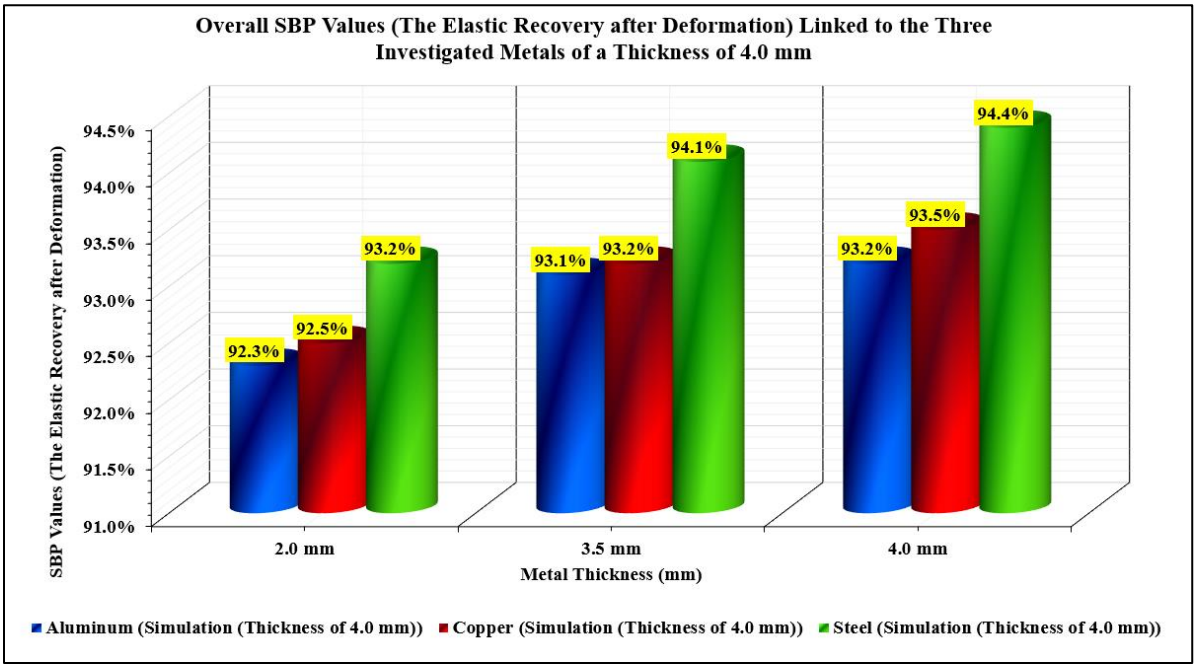

Figure ١٦. The SBP (the elastic recovery ratio) of the three metals of a thickness of ٤,٠ mm.

It can be understood from the graphical comparative analysis explained in Figure ١٦ that the mathematical simulations affirmed, a second time, that the pure steel specimens of thicknesses of ٢,٠ mm, ٣,٥ mm, and ٤,٠ mm did exhibit significantly large elastic recovery percentage after deformation occurred after the mold loading was removed in comparison to copper and aluminum. Contrastingly, the aluminum specimens have lower elastic recovery after removing the mold load (٩٣,١٪ and ٩٣,٢٪ at thicknesses of ٣,٥ mm and ٤,٠ mm). Copper has closer elastic recovery ratio to that of aluminum at a thickness of ٢,٠ mm, corresponding to ٩٢,٥٪ and ٩٢,٣٪, respectively.

As seen in previous figures, pure steel did also record the highest elastic recovery ratio compared with copper and aluminum. It reaches its maximum elastic recovery ratio (٩٤,٤٪) when its specimen thickness was ٤,٠ mm. Correspondingly, a conclusion can be reached that manufacturing companies and automobile engineers can exploit pure steel due to its consistent exhibition of the highest elastic recovery (SBP) percentage across all metal thicknesses. Aluminum shows the lowest elastic recovery ratios, except at ٢,٠ mm where it approximates the SBP behavior of copper. For this reason, this figure can confirm the superior elastic recovery of pure steel amidst deformation conditions after removing the mold loading.

٦. Discussion

٦,١ *The Effect of Punch Radius on SBP*

The influence of punch radius on SBP value is studied. In the FEA simulations and the experiment, the punch radii were ٢,٠ mm, ٣,٥ mm, and ٤,٠ mm. The obtained results through simulations provided some critical insights on the influence of punch radii on the SBP of pure aluminum, pure copper, and pure steel. It was distinguished that the SBP value (elastic recovery percentage) would increase after removing the applied mold loading as the punch die radius increases. The SBP relies on the size of the plastic deformation zone.

A punch with a small radius concentrates the pressure force within a narrow space, resulting in higher local stress and more plastic deformation. As the punch radius increases, the force spreads to a large plastic area; thus, increasing the SBP.

In other words, as the punch radius increases, the contact angle and contact area would increase. As a result, this phenomenon can create more friction surface between the punch and the sheet. So, it is obvious that SBP ratios would increase with increasing the punch radius. Pure steel and copper exhibit larger elastic recovery ratios after removing the mold load than aluminum across all thicknesses. This can happen because with greater punch radii of the contact area between the punch and the sheet would become greater. As a result, the bending moment would escalate, causing a larger spring back angle.

These outcomes are consistent with Wu (١٩٩٦), who exploited virtual forming model after implementing spring-forward simulations. Deformable part mesh became rigid. The study investigated the impacts of the virtual die and punch dimensions. It was found that the die shape and dimensions would have significant impact on the SBP of the metal. Also, the metal's punch radius has significant effect on the elastic recovery ratio of the material, relying on FEA.

The corresponding metal's dimensions impacts on the SBP of the steel were also examined and confirmed by the Slota *et al*. (٢٠١٣) research, who explained that optimization of the die radius, SBP angle, and critical dimensions of some investigated metals, specifically high-

strength steel and lightweight alloys, play a crucial role in modifying and amending the behavior of SBP in these metals.

These results are also compatible with the study conducted by Şen and Taşdemir (٢٠٢١), who found that SBP would lessen with greater values of the die angle. They noticed that SBP would increase with larger values of the punch radius under limited mold load application time.

٦،٢ *Effect of Sheet Metal Type*

From the FEA simulations, it was found that the three sheet metal thickness values of ٢ mm, ٣،٥ mm, and ٤ mm linked to the three metals, which are aluminum, copper, and pure steel did exhibit different behaviors of SBP and corresponded to various elastic recovery percentages. To explain, the relation between the SBP and material properties was found to have some considerable effects linked to the materials' applicability in production. For ductile materials, the SBP ratio is much lower than in hard metals, with dependence on the modulus of elasticity (Young's modulus) of a particular material.

The amount of SBP rises with greater yield strength materials. For instance, aluminum, copper, and pure steel could exhibit different ranges of SBP characteristics. The obtained analytical results of SBP radius of wiping die bending sheet metal are different for these three metals, aluminum, copper, and pure steel. The aluminum has lower ratios of SBP/ elastic recovery percentage than the other two metals, copper, and pure steel. When the SBP bending radius increases, the material would show more SBP than the lower bend radius.

In conclusion, it was discovered that the SBP would lessen from pure steel across copper to aluminum.

These results are compatible with the findings of Özdemir (٢٠٢٠), who did also investigated the SBP behavior and elastic recovery in the Dp-٦٠٠/ dual-phase steel sheet metal on which a V-mold loading was applied. The author did affirmed the effect of a collection of variables on the SBP of the Dp-٦٠٠/ dual-phase steel, including various values of bending variables, like the punch tip radii, sheet thicknesses, and other model geometrical characteristics and dimensions. Thus, the researcher exploited signal-to-noise ratio to make careful choice and optimization concerning the best rates of each index.

Moreover, the results regarding the effect of the sheet metal type were consistent with the mathematical simulation outcomes of Lafta *et al*. (٢٠٢٠), who studied the SBP in copper and aluminum relying on V-shape mold loading. The scholars found that the change of die radii, punch radii, metals' thicknesses could affect the behavior of the SBP, elastic recovery, and strain profile.

٧. Conclusions

The research in this article was conducted to distinguish the impacts of a number of geometry variables of sheet metal models on their SBP behavior, performance, strain, and elastic recovery after deformation occurs after the applied mold load is removed. To achieve the study objectives a mathematical simulation process was implemented after formulating three sheet metal models, including aluminum, copper, and pure steel. V-shape mold was created in the SolidWorks software and exported to the ANSYS software tool through which corresponding mathematical simulations were performed to these three metals under careful section of

thicknesses and punch radii. Relying on the numerical primary data collection and analysis of, the substantial research findings can be listed in the following points:

A- The SBP value (elastic recovery percentage) would increase after removing the applied mold loading as the punch die radius increases. The SBP relies on the size of the plastic deformation zone,

B- A punch with a small radius concentrates the pressure force within a narrow space, resulting in higher local stress and more plastic deformation. As the punch radius increases, the force spreads to a large plastic area; thus, increasing the SBP,

C- As the punch radius increases, the contact angle and contact area would increase. As a result, this phenomenon can create more friction surface between the punch and the sheet.

D- SBP ratios would increase with increasing the punch radius. Pure steel and copper exhibit larger elastic recovery ratios after removing the mold load than aluminum across all thicknesses.

E- Greater punch radii of the contact area between the punch and the sheet would become greater. As a result, the bending moment would escalate, causing a larger spring back angle,

F- For ductile materials, the SBP ratio is much lower than in hard metals, with dependence on the modulus of elasticity (Young's modulus) of a particular material,

G- The amount of SBP rises with greater yield strength materials. Aluminum, copper, and pure steel could exhibit different ranges of SBP characteristics,

H- The aluminum has lower ratios of SBP/ elastic recovery percentage than the other two metals, copper, and pure steel. When the SBP bending radius increases, the material would show more SBP than the lower bend radius.

CRediT Authorship Contribution Statement:

Elham: Writing, Review and Editing, Mechanical Engineering Investigation, Numerical Analysis, Mathematical Simulations, Data Analysis, Conceptualization, Methodology.

Declaration of competing interest

The authors declare that they have no known competing financial interests or personal relationships that could have appeared to influence the work reported in this paper.

Acknowledgements

The researcher would like to acknowledge academic experts and mechanical engineering consultants, who did take a role in examining, reading, validating, and estimating the entire numerical study findings of this research.

References

Asgari, S. A., Pereira, M., Rolfe, B. F., Dingle, M., & Hodgson, P. D. (٢٠٠٨). Statistical analysis of finite element modeling in sheet metal forming and spring back analysis. Journal of materials processing technology, ٢٠٣(١-٣), ١٢٩-١٣٦.

Baùon, P., Úwiàtoniowski, A., & Szostak, J. (٢٠١٦). Improved method of spring back compensation in metal forming analysis. Strength of Materials, ٤٨, ٥٤٠-٥٥٠.

Broggiato, G. B. (٢٠١٢). Finite element simulation of spring back in sheet metal forming processes. *International Journal of Mechanical Sciences*, *57*(١), ٥٥-٦٦.

Chen, L. (٢٠١١). Finite element simulation of spring back in sheet metal forming. Applied Mechanics and Materials, ٥٠, ٦١٥-٦١٨.

Choi, Y., Lee, J., Panicker, S. S., Jin, H. K., Panda, S. K., & Lee, M. G. (٢٠٢٠). Mechanical properties, spring back, and formability of W-temper and peak aged ٧٠٧٥ aluminum alloy sheets: Experiments and modeling. International Journal of Mechanical Sciences, ١٧٠, ١٠٥٣٤٤.

Dametew, A. W., & Gebresenbet, T. (٢٠١٦). Numerical investigation of spring back on sheet metal bending process. Global J Res Eng: Mech Mech Eng, ١٦(٤).

Guo, Q., Yao, W., Li, W., & Gupta, N. (٢٠٢١). Constitutive models for the structural analysis of composite materials for the finite element analysis: A review of recent practices. *Composite Structures*, *260*, ١١٣٢٦٧.

Helmy, M. A. (٢٠١٩). Numerical investigation of spring back prediction in metal forming. *Journal of Engineering Sciences*, *47*(٣), ١-١٠.

Jiang, H., & Li, G. (٢٠١٥). Spring back simulation and compensation in sheet metal forming using finite element method. *International Journal of Mechanical Sciences*, *101*, ٣٢-٤٠.

Jin, S., Li, Z., Gao, T., Huang, F., Gan, D., & Cheng, R. (٢٠٢١). Constrained shell finite element method of modal buckling analysis for thin-walled members with curved cross-sections. *Engineering Structures*, *240*, ١١٢٢٨١.

Katre, S., Karidi, S., Durga Rao, B., Ramulu, P. J., & Narayanan, R. G. (٢٠١٥). Spring back and formability studies on friction stir welded sheets. In Advances in Material Forming and Joining: ٥th International and ٢٦th All India Manufacturing Technology, Design and Research Conference, AIMTDR ٢٠١٤ (pp. ١٤١-١٦٥). Springer India.

Kim, D. Y., Hwang, B. K., Lee, Y. S., Kim, S. W., & Moon, Y. H. (٢٠١٠). Influence of Annealing Treatment on Formability and Spring back for Magnesium Alloy Sheets. Key Engineering Materials, ٤٤٣, ١٨٩-١٩٤.

Kurowski, P. M. (٢٠٢٢). *Finite element analysis for design engineers*. Reading: Textbook. Publisher: SAE International.

Özdemir, M. (٢٠٢٠). Optimization of spring back in air v bending processing using Taguchi and RSM method. *Mechanics*, *26*(١), ٧٣-٨١.

Pagani, A., Azzara, R., Augello, R., & Carrera, E. (٢٠٢١). Stress states in highly flexible thin-walled composite structures by unified shell model. *AIAA Journal*, *59*(١٠), ٤٢٤٣-٤٢٥٦.

Saravanan, S., Saravanan, M., & Jeyasimman, D. (٢٠١٨). Study on effects of spring back on sheet metal bending using simulation methods. International journal of mechanical and production, ٨, ٩٢٣-٩٣٢.

Slota, J., & Jurčišin, M. (٢٠١٢). Experimental and Numerical Prediction of Spring back in V-Bending of Anisotropic sheet metals for automotive industry. Zeszyty Naukowe Politechniki Rzeszowskiej. Mechanika, (٨٤ [٢٨٤], nr ٣), ٥٥-٦٨.

Szabó, B., & Babuška, I. (٢٠٢١). Finite element analysis: Method, verification and validation. Reading: Textbook. Publisher: John Wiley & Sons.

Toros, S., Ozturk, F., & Kacar, I. (٢٠١٢). Review of warm forming of aluminum-magnesium alloys. *Journal of Materials Processing Technology*, *207*(١-٣), ١-١٢.

Vrh, M., Halilovič, M., Starman, B., & Štok, B. (٢٠٠٩). Modelling of spring back in sheet metal forming.

Wu, L. (١٩٩٦). Generate tooling mesh by FEM virtual forming model for spring back compensation Toros, S., Polat, A., & Ozturk, F. (٢٠١٢). Formability and spring back characterization of TRIP٨٠٠ advanced high strength steel. Materials & Design, ٤١, ٢٩٨-٣٠٥.

Xu, W. L., Ma, C. H., Li, C. H., & Feng, W. J. (٢٠٠٤). Sensitive factors in spring back simulation for sheet metal forming. Journal of Materials Processing Technology, ١٥١(١-٣), ٢١٧-٢٢٢.